EFFECT OF THERMAL RADIATION ON NATURAL CONVECTION OF A NANOFLUID IN A SQUARE CAVITY WITH A SOLID BODY

by

***Sayyedah A. QASEM*[a], *Sivanandam SIVASANKARAN*[b], *Zailan SIRI*[a*], and *Wan A. M. OTHMAN*[a]**

[a]Institute of Mathematical Sciences, Faculty of Science, University Malaya, Kuala Lumpur, Malaysia
[b]Department of Mathematics, King Abdulaziz University, Jeddah, Saudi Arabia

Original scientific paper
https://doi.org/10.2298/TSCI191003182Q

This investigation is to concentrate on the effect of thermal radiation on free convection of a Cu-water nanofluid in a differentially heated cavity containing a solid square block placed in the middle. The upper and lower dividers of the cavity are kept as thermally protected; The coupled equations of mass, momentum, and energy are governed the mathematical model. Finite difference method is used to solve the governing equations. All internal surfaces of the cavity are deemed as a diffused emitters and reflectors for radiation. The impacts of relevant parameters, the Rayleigh number ($10^3 \leq Ra \leq 10^6$), volume fraction of nanoparticles ($0.0 \leq \phi \leq 0.04$) and thermal radiation (Rd = 0, 1, 5, and 10), are explored. For various values of the flow parameters, the values for local and average Nusselt number are calculated. It is observed that the local and averaged Nusselt numbers are increased with an increase in the Rayleigh number and volume fraction of nanoparticles. Also, the temperature distribution of the fluid increases with an increase in the radiation parameter.

Key words*: natural convection, nanofluid, Rayleigh number, finite difference method, thermal radiation*

Introduction

The influence of thermal radiation on natural convection of a nanofluid in cavities containing solid body is one of the thrust areas of contemporary research due to their wide potential regarding the development of heat transfer. The term 'nanofluid' initially proposed by Choi and Eastman [1]. Nanofluid has acquired significant attention in current years because of the easy production technique and inexpensive price. Additionally, the thermal conductivity of nanofluids comparative to the base fluids is high. As a result, nanofluids play an important role in several energy-related systems applications such as radiators, heat exchangers, cooling and heating in buildings, solar collectors, home ventilation, medical applications that attract many researchers. Thus, the increase in research activities regarding convection heat transfer is significant. At high temperatures, several engineering processes occur and hence the knowledge of radiation heat transfer in the cavities having a solid body is a vital

* Corresponding author, e-mail: zailansiri@um.edu.my

thing that is required for designing appropriate equipment. Several works could be addressed for the convection heat transport in cavities at different geometries and orientations [2-5]. Choeng *et al*. [6] studied the free convective flow and transfer of heat in a sinusoidally heated wavy porous enclosure in the existence of inner heat generation or absorption. The results presented that the rate of heat transfer in the enclosure decreases by an increase in the internal heat generation/absorption parameter.

Nanofluid is one of the most highlighted topics for the recent research since it enables to increase the Nusselt number. Hence, the small thermal conductivity of the water, oil, and other fluids is the main issue to realize more heat transfer rate. Nanofluid is a blend of fluid as a base fluid which includes scattered solid nanoparticles, hence nanoparticles big thermal conductivity corresponds to the higher thermal conductivity of the mixture. Recently, various researchers considered the influence of nanoparticles through several models of liquid [7-9]. Hayat *et al*. [10] studied the steady mixed convective flow of Cu- and Ag-water nanofluid by rotating the disk of variable thickness. Also, they have considered the impacts of the Jole heating and thermal radiation with the additional influences of viscous dissipation. To improve the solutions, the homotopy analysis method is applied. The main conclusions found have been presented. Khanafer *et al*. [11] introduced the buoyancy-driven heat transfer enhancement in a 2-D cavity loaded with nanofluid. With the use of finite-volume method along with the alternating direct implicit procedure, the transport equations were solved numerically, as well as the heat transfer allocation along with the thermal conductivity enhancement was studied. It was observed that the nanoparticles strong enhancement was created on the rate of heat transfer for all Grashof number values. Sivasankaran *et al*. [12] investigated the convective flow and heat transfer of nanofluids with different nanoparticles in a square cavity. The transport equations were discretised using the finite volume approach, which solved by iterative technique. It was found that the rate of heat transfer increment when the nanoparticles volume fraction is increased. Tiwari and Das [13] explored the heat transfer augmentation of the nanofluid inside two-sided lid-driven square enclosure. With finite volume method employing SIMPLE algorithm, numerically the transport equations were solved. They have considered three cases in the direction of the motion walls, as well as the effect of the Richardson number. It is observed that both the direction of the moving walls and the Richardson number impact the heat transfer and fliud-flow in the enclosure. Recently, Cattaneo-Christov heat flux model is utilized to improve the energy equations by many researchers [14-16]. Magnetic field has many uses in industry. Power generators, purification of metals, electrostatic precipitation are some applications of MHD fluids. In addition, can use MHD to control the rate of cooling and boundary-layer thickness. Different studies were made to investigate flow conduct over an extended surface under MHD. One may refer few [17-23] in this direction.

This research reveals that the exchange of radiation homogenizes the temperature in the enclosure and resulting in an increment in the mean Nusselt number, especially when the ration of the solid/fluid and the Rayleigh number are high. Not only that but also the average of the Nusselt number is getting increased by the increasing emissivity of the radiative surfaces especially when Rayleigh number at a high rate. The outcomes of other several numerical simulations in cavities and tubes of free, force and mixed convection of nanofluid, it has been found that imply its positive effect on Nusselt number. Various numerical studies have been conducted in nanofluid and heat transfer [24-28]. However, the next case which led to achieving more accurate findings comparing experimental ones was the coupled free convection with radiation heat transfer, several papers studied the influence of surface radiation on free convection [29-31]. Ridouane *et al*. [32, 33] examined the effect of thermal radiation on natural convection in a heated enclosure. It was noticed that thermal radiation affected the rate of heat transition from the horizontal walls. It is observed that the surface thermal radiation contribution on natural convection of a nanofluid is negligent in most of the previous papers which could cause some detours in findings [34, 35].

Based on the previously mentioned investigations and to the best knowledge of the authors, the influence of thermal radiation on free convection of a Cu-water nanofluid in a differentially heated cavity containing a solid square is a problem that yet to be investigated. Hence, the aim of this study to concentrate on the influence of thermal radiation on free convection of a Cu-water nanofluid in a differentially heated cavity with a solid block inserts. A square cavity with different temperature distributions is significant issues in the applications of the thermal processing, for instance, in transport and drying of gases, enhanced oil recovery by hot water flooding, molten metals infiltration and combustion of heavy oils. Hence, the authors believe that the current study is a valuable contribution to developing heat transfer enhancement and thermal performance in some engineering devices.

Mathematical formulation

A schematic diagram of the 2-D square cavity with width and height, H, containing an insulated object of height, ly, and width, lx ($ly = lx = 0.2$) centered as shown in fig. 1, which provided the physical configuration of the present issue. The left and right walls of the outer cavity have constant but various temperatures, T_h and T_c, respectively. The top and bottom walls of the enclosure are considered perfectly isolated. The cavity is filled with nanofluid of Cu-water. The velocities, u and v, are defined in, x and y, directions, respectively. The gravity acts in the downward trend.

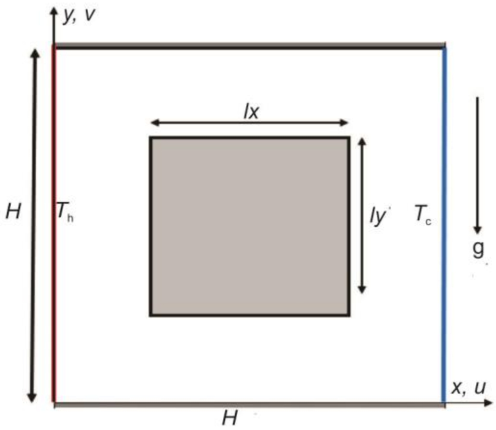

Figure 1. A schematic perspective of the enclosure

The thermophysical characteristics of the nanofluid are supposed to be steady excluding its density variation in the duration of buoyancy by Boussinesq approximation. Furthermore, the current study assumes that the dissipate of the glutinous is ignored. The continuity, momentum and energy equations for 2-D natural convection fluid-flow and heat transfer of the nanofluids in the enclosure are given by:

$$\frac{\partial u}{\partial x}+\frac{\partial v}{\partial y}=0 \tag{1}$$

$$u\frac{\partial u}{\partial x}+v\frac{\partial u}{\partial y}=-\frac{1}{\rho_{\rm nf}}\frac{\partial P}{\partial x}+\frac{\mu_{\rm nf}}{\rho_{\rm nf}}\left(\frac{\partial^2 u}{\partial x^2}+\frac{\partial^2 u}{\partial y^2}\right) \tag{2}$$

$$u\frac{\partial v}{\partial x}+v\frac{\partial v}{\partial y}=-\frac{1}{\rho_{\rm nf}}\frac{\partial P}{\partial y}+\frac{\mu_{\rm nf}}{\rho_{\rm nf}}\left(\frac{\partial^2 v}{\partial x^2}+\frac{\partial^2 v}{\partial y^2}\right)+\frac{(\rho\beta)_{\rm nf}}{\rho_{\rm nf}}{\rm g}\left(T-T_{\rm c}\right) \tag{3}$$

$$u\frac{\partial T}{\partial x}+v\frac{\partial T}{\partial y}=\alpha_{\rm nf}\left(\frac{\partial^2 T}{\partial x^2}+\frac{\partial^2 T}{\partial y^2}\right)+\frac{1}{(\rho c_p)_{\rm nf}}\left(\frac{\partial q_r}{\partial x}+\frac{\partial q_r}{\partial y}\right) \tag{4}$$

The heat flux due to radiation along x and y directions are given by:

$$q_r = \frac{-4\sigma^*}{3K'}\frac{\partial T^4}{\partial x} \quad \text{and} \quad q_r = \frac{-4\sigma^*}{3K'}\frac{\partial T^4}{\partial y}$$

The temperature difference inside the flow is supposed to be very small via approximation of Rooseland for thermal radiation. By the use of Taylor series, T^4, is approximated:

$$T^4 \cong 4T_\mathrm{c}^3 T - 3T_\mathrm{c}^4$$

and so, the heat flux due to radiation along the horizontal and vertical direction becomes:

$$q_r = \frac{-16\sigma^* T_0^3}{3K'}\frac{\partial T}{\partial x} \quad \text{and} \quad q_r = \frac{-16\sigma^* T_0^3}{3K'}\frac{\partial T}{\partial y}$$

The boundary conditions for physical model:

$$\begin{array}{lcl}
\text{on each solid boundaries} & : & u = v = 0 \\
\text{on } x = 0, \ 0 \le y \le \mathrm{H} & : & T = T_\mathrm{h} \\
\text{on } x = H, \ 0 \le y \le H & : & T = T_\mathrm{c} \\
\text{on } Y = 0, \ Y = H, \ 0 \le x \le H & : & \dfrac{\partial T}{\partial Y} = 0
\end{array}$$

By employing the below dimensionless parameters, the governing equations could be converted to dimensionless form:

$$X = \frac{x}{H}, \ Y = \frac{y}{H}, \ V = \frac{vH}{\alpha_\mathrm{f}}, \ U = \frac{uH}{\alpha_\mathrm{f}}, \ P = \frac{pH^2}{\rho_\mathrm{nf}\alpha_\mathrm{f}^2}, \ \Theta = \frac{T - T_\mathrm{c}}{T_\mathrm{h} - T_\mathrm{c}}, \ \mathrm{Pr} = \frac{\nu_\mathrm{f}}{\alpha_\mathrm{f}}$$
$$\Psi = \frac{\psi \,\mathrm{Pr}}{v}, \ \Omega = \frac{\omega H^2 \,\mathrm{Pr}}{v}, \ \mathrm{Ra} = \frac{\mathrm{g}\beta_\mathrm{f}(T_\mathrm{h} - T_\mathrm{c})H^3}{\alpha_\mathrm{f}\nu_\mathrm{f}}, \ Rd = \frac{4\sigma^* T_\mathrm{c}^3}{k_\mathrm{f} K'} \tag{5}$$

Dimensionless forms of the governing equations are:

$$\frac{\partial U}{\partial X} + \frac{\partial V}{\partial Y} = 0 \tag{6}$$

$$U\frac{\partial U}{\partial X} + V\frac{\partial U}{\partial Y} = -\frac{\partial P}{\partial X} + \frac{\mu_\mathrm{nf}}{\rho_\mathrm{nf}\alpha_\mathrm{f}}\left(\frac{\partial^2 U}{\partial X^2} + \frac{\partial^2 U}{\partial Y^2}\right) \tag{7}$$

$$U\frac{\partial V}{\partial X} + V\frac{\partial V}{\partial Y} = -\frac{\partial P}{\partial X} + \frac{\mu_\mathrm{nf}}{\rho_\mathrm{nf}\alpha_\mathrm{f}}\left(\frac{\partial^2 V}{\partial X^2} + \frac{\partial^2 V}{\partial Y^2}\right) + \frac{(\rho\beta)_\mathrm{nf}}{\rho_\mathrm{nf}\beta_\mathrm{f}}\mathrm{Ra}\,\mathrm{Pr}\,\Theta \tag{8}$$

$$U\frac{\partial \Theta}{\partial X} + V\frac{\partial \Theta}{\partial Y} = \frac{\alpha_\mathrm{nf}}{\alpha_\mathrm{f}}\left(1 + \frac{4k_\mathrm{f}}{3k_\mathrm{nf}}Rd\right)\left(\frac{\partial^2 \Theta}{\partial X^2} + \frac{\partial^2 \Theta}{\partial Y^2}\right) \tag{9}$$

The boundary conditions of equations as:

$$\begin{array}{lcl}
\text{on the left} & : & U = V = 0, \ \Theta = 1 \\
\text{on the right wall} & : & U = V = 0, \ \Theta = 0 \\
\text{on the insulated object} & : & U = V = 0, \ \dfrac{\partial \Theta}{\partial n} = 0
\end{array} \tag{10}$$

The vorticity and stream functions are taken as:

$$U = \frac{\partial \Psi}{\partial Y}, \quad V = -\frac{\partial \Psi}{\partial X}, \quad \frac{\partial^2 \Psi}{\partial X^2} + \frac{\partial^2 \Psi}{\partial Y^2} = -\Omega \tag{11}$$

Using eqs. (11) and (5), the equations of governing and the conditions of the boundary (10) with respecting to the dimensionless parameters are:

$$\frac{\partial^2 \Psi}{\partial X^2} + \frac{\partial^2 \Psi}{\partial Y^2} = -\Omega \tag{12a}$$

$$\frac{\partial^2 \Omega}{\partial X^2} + \frac{\partial^2 \Omega}{\partial Y^2} = \frac{\rho_{\mathrm{nf}} \alpha_{\mathrm{nf}}}{\mu_{\mathrm{nf}}} \left[\left(\frac{\partial \Psi}{\partial Y} \frac{\partial \Omega}{\partial X} - \frac{\partial \Psi}{\partial X} \frac{\partial \Omega}{\partial Y} \right) - \frac{(\rho\beta)_{\mathrm{nf}}}{\rho_{\mathrm{nf}}} \mathrm{Ra}\,\mathrm{Pr} \frac{\partial \Theta}{\partial X} \right] \tag{12b}$$

$$\frac{\partial^2 \Theta}{\partial X^2} + \frac{\partial^2 \Theta}{\partial Y^2} = \frac{\alpha_{\mathrm{f}}}{\alpha_{\mathrm{nf}}} \left(\frac{3k_{\mathrm{nf}}}{3k_{\mathrm{nf}} + 4k_{\mathrm{f}} Rd} \right) \left(\frac{\partial \Psi}{\partial Y} \frac{\partial \Theta}{\partial X} - \frac{\partial \Psi}{\partial X} \frac{\partial \Theta}{\partial Y} \right) \tag{13}$$

$$U \frac{\partial \Theta}{\partial X} + V \frac{\partial \Theta}{\partial Y} = \frac{\alpha_{\mathrm{nf}}}{\alpha_{\mathrm{f}}} \left(1 + \frac{4k_{\mathrm{f}}}{3k_{\mathrm{nf}}} Rd \right) \left(\frac{\partial^2 \Theta}{\partial X^2} + \frac{\partial^2 \Theta}{\partial Y^2} \right) \tag{14}$$

under the conditions of the constraint:

$$\begin{aligned}
&\text{on the solid walls} &&: \quad \Psi = 0 \\
&\text{on } x = 0, \quad 0 \le y \le 1 &&: \quad \Theta = 1, \quad \Omega = -\frac{\partial^2 \Psi}{\partial X^2} \\
&\text{on } x = 1, \quad 0 \le y \le 1 &&: \quad \Theta = 0, \quad \Omega = -\frac{\partial^2 \Psi}{\partial X^2} \\
&\text{on } Y = 0, \quad Y = 1, \quad 0 \le X \le 1 &&: \quad \frac{\partial \Theta}{\partial Y} = 0, \quad \Omega = -\frac{\partial^2 \Psi}{\partial X^2}
\end{aligned} \tag{15}$$

The general heat transition through the enclosure is an important parameter in the applications of the engineering. The local and averaged Nusselt number is calculated on the walls by employing:

$$\mathrm{Nu} = \left[-\frac{k_{\mathrm{nf}}}{k_{\mathrm{f}}} \left(1 + \frac{4k_{\mathrm{f}}}{3k_{\mathrm{nf}}} Rd \right) \frac{\partial \Theta}{\partial X} \right] \tag{16}$$

$$\overline{\mathrm{Nu}} = \int_0^1 \mathrm{Nu}\, \mathrm{d}Y \tag{17}$$

Solution procedure

The eqs. (12)-(14) undergo to the boundary conditions (15) are solved by using the finite difference method. The stream function (12) is solved by employing the successive over-relaxation method while the vorticity eq. (13) and energy eq. (14) are solved by utilizing the Gauss-Seidel iterative method. In this work, uniform grids in *X*- and *Y*- directions are using in all computational proceedings. The grid of 101 × 101 has been taken for the computations. A converged solution is gotten via employing the relation:

$$\Xi = \sum_{i,j} \left(\zeta_{i,j}^{n+1} - \zeta_{i,j}^{n} \right) < 10^{-6}$$

where ζ is either Ψ, Ω, or Θ.

The Nusselt number over the side-wall has calculated via employing the forward difference approximation and the numerical integration (*i.e*. trapezoidal rule) is using to calculate the averaged Nusselt number at the side walls. Indeed, in the previous literature, the code of the performed computerized is validated via utilizing a heated square cavity with a constant temperature at the left side.

The comparison of some findings for free convection in a square cavity is tabulated in tab.1. From tab.1, the findings predicted by current computer code are agreed well with the previous studies.

Table 1. Comparison of $\overline{\mathrm{Nu}}$ findings for free convection in a square enclosure

References	Mesh Size	Ra = 10^3	Ra = 10^4	Ra = 105	Ra = 10^6
De Vahl Davis and Jones [36]	81 × 81	1.118	2.243	4.519	8.800
Bilgen and Yedder [37]	60 × 60	–	–	–	–
Ho *et al*. [38]	81 × 81	1.118	2.246	4.522	8.825
Cheong *et al*. [39]	111 × 111	1.118	2.246	4.526	8.844
Present study	111 × 111	1.1161	2.2468	4.5253	8.8436

Results and discussion

The effect of thermal radiation on free convection of nanofluid composed of Cu-water inside a differentially heated enclosure containing an insulated square placed at the centre is simulated numerically by applying the finite difference method. It is eligibility to say that the interaction among radiation and assumed nanofluid natural convection inside a differentially heated cavity having a solid square block is investigated for the first time in the current study.

Effects of the thermal radiation parameter and nanoparticles volume fraction ($\phi = 0.0$) and ($\phi = 0.04$) on the flow pattern and temperature dissemination inside the enclosure with a solid square body with aspect ratio (dimensionless size) $lx = ly = 0.2$,are depicted for Ra = 10^4 in figs. 2 and 3, respectively. The streamlines are placed close to the isothermal side walls and distinct velocity boundary-layers are formed at $Rd = 0$ and for the values of ϕ. Two secondary eddies are developed in the lower left and upper right sides of the solid square body for the cavity filled with pure fluid and nanofluid.

The flow intensity increases and the streamlines move closer to the side walls by increase of the buoyant force via increase in the thermal radiation parameter. For the cavity filled with pure fluid and nanofluid, heat transfer of the isotherms are nearly parallel with the vertical walls via domination of conduction, at Ra = 10^4 and for all values of thermal radiation excepted for $Rd = 0$. A from the streamlines, single clockwise eddy is observed inside the cavity. The symmetric eddy indicates a low velocity and low-intensity flow at low thermal radiation parameter. The same behaviour is found for the cavities filled with nanofluid from the streamlines. The effect of free convection escalation and the isotherms are condensed next to the isothermal side walls with increase in the thermal radiation parameter. Furthermore, the left and right sides of the square body implies the thermal stratification. From the isotherms at $Rd = 0$, formation of the thermal boundary-layers can be observed. At each thermal radiation parameter, it is visible from the isotherms that with increase in the nanoparticles volume fraction, the thermal boundary-layers thicken via increase in the thermal conductivity of the nanofluid, reduction of the temperature gradient adjacent to the side walls and escalation in the diffusion of heat.

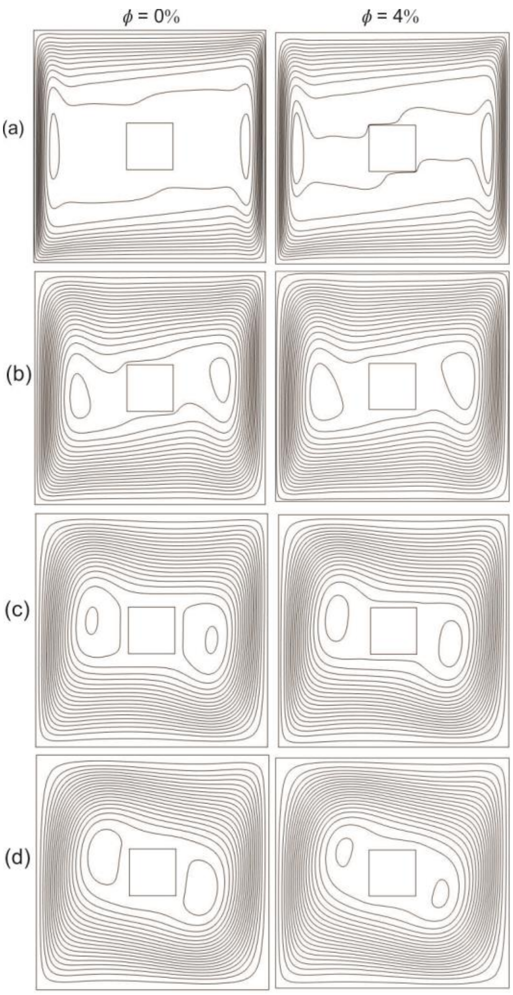

Figure 2. Streamlines for different values of (a) Rd = 0, (b) Rd = 1, (c) Rd = 5, and (d) Rd = 10 with ϕ = 0% and ϕ = 4 % at Ra = 10^6

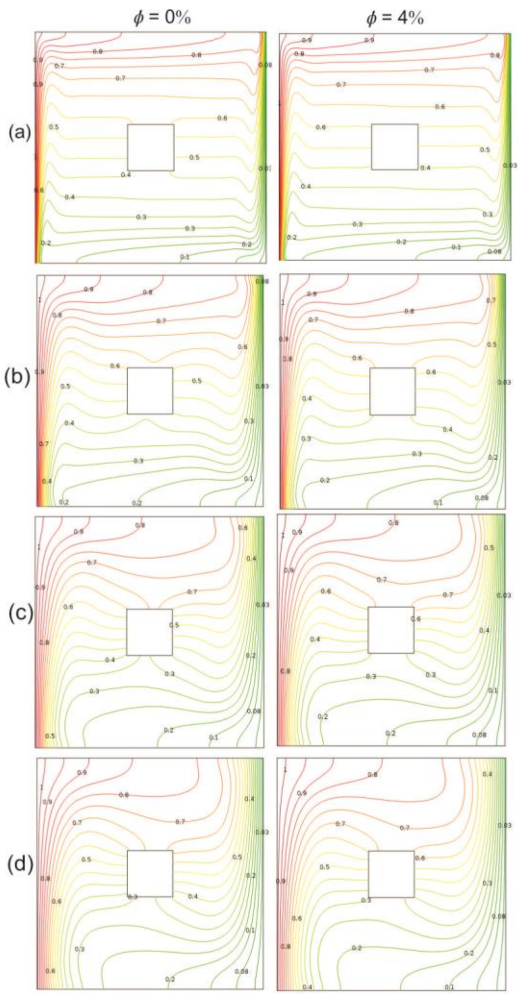

Figure 3. Isotherms for different values of (a) Rd = 0, (b) Rd = 1, (c) Rd = 5, and (d) Rd = 10 with ϕ = 0% and ϕ = 4 % at Ra = 10^6

Variation of the local number of Nusselt with the volume fraction of the nanoparticles (ϕ = 0.0, 0.01, and 0.04) at the Rayleigh numbers Ra = 10^6 and different radiation parameter, are displayed in fig. 4. We can conclude that the transfer of heat is rising with an increase in the radiation parameter and Rayleigh number. Moreover, we can note that the change in the volume fraction of the nanoparticles does not impact the heat transfer significantly.

At various values of the thermal radiation parameter for all volume fraction of the nanoparticles at Ra = 10^3 and Ra = 10^6, it could be seen from fig. 5(a) at Ra = 10^3 the lower end of the hot wall happens the maximum local Nusselt number. At this area, the cold fluid visage the hot wall; thus, maximum gradient of temperature happens at this zone. When the fluid increments close to the hot side the temperature of the fluid raises, hence the gradient of the temperature decreases, thus the local Nusselt number decreases too. For ϕ = 0.02 at the upper part of the hot wall occurs minimum local Nusselt number. In addition, for this value of the nanoparticles volume fraction, regular distribution of the Nusselt number is noticed over the whole upper half of the hot side.

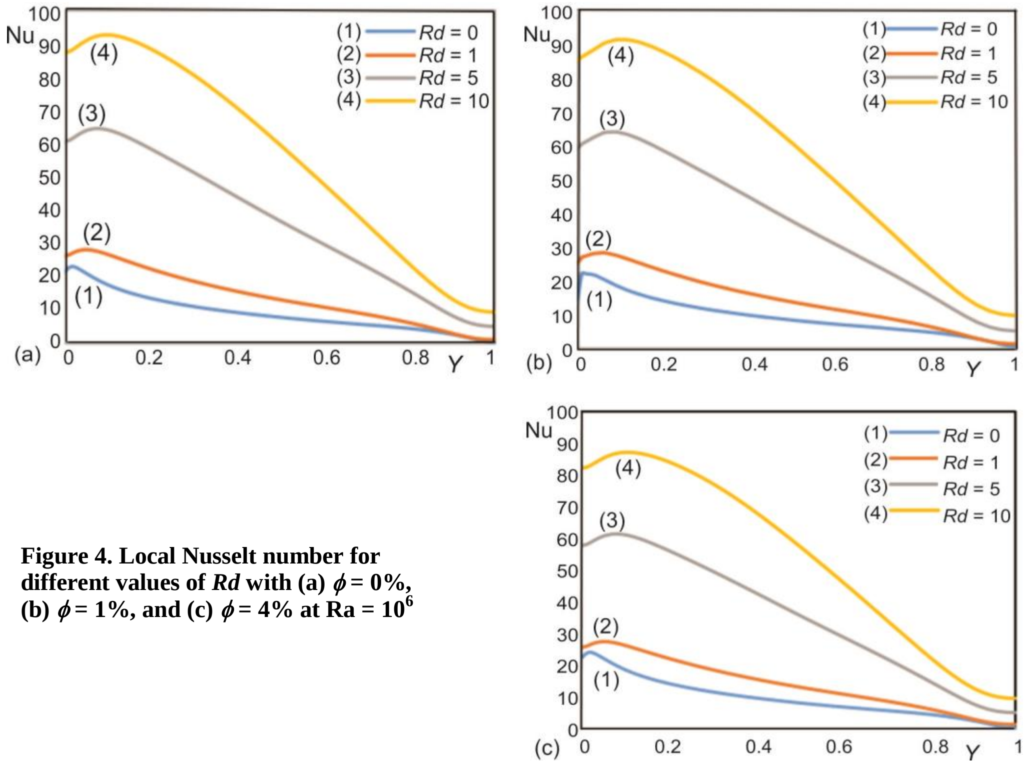

Figure 4. Local Nusselt number for different values of *Rd* with (a) $\phi = 0\%$, (b) $\phi = 1\%$, and (c) $\phi = 4\%$ at Ra = 10^6

At Ra = 10^6 and *Rd* = 0 numbers, the maximum heat transfer rate happens of the hot wall at the lower end. Maximum local Nusselt number of the hot wall at the lower end happen for the enclosure with $\phi = 0.04$. The local Nusselt number decreases when the nanoparticles volume fraction increases.

At figs. 5(b) and 5(c) with Ra = 10^6, the nanoparticles volume fraction does not influence the distribution of the Nusselt number significantly.

From fig. 5(c) at Ra = 10^3 the various behaviour is noticed. At this Rayleigh number for the enclosure with thermal radiation (*Rd* = 10), the increment in the volume fraction of the nanoparticles does not influence the distribution of the local Nusselt number significantly. With the increment in the radiation parameter, the influence of the volume fraction nanoparticles on the local Nusselt number raises, when the Rayleigh number is 10^3.

Variations of the Nusselt number average with respect to the nanoparticles volume fraction for various values of the radiation parameter at various Rayleigh numbers are provided in fig. 6. The heat transfer rate rises with the increment in the nanoparticles volume fraction for all values of Rayleigh numbers. In additionally, a radiation value *Rd* = 10 grants better Nusselt Number, pursued by *Rd* = 5. The gap becomes so important, due to the highest radiation convection heat transition rate, for the high Rayleigh numbers.

Figure 7 presents the variation of the average Nusselt number with the Radiation parameter, at various Rayleigh numbers. The provided outcomes in this figure are for the various values of the volume fraction of the nanoparticles. As noted from the figure, transfer of heat raises monotonically with the rise of the values of radiation parameter for all Rayleigh number. At the lower Rayleigh number Ra = 10^3, the lowest transfer of heat was noticed for (ϕ = 0.0). As the values of the radiation parameter rise, the variance for the Nusselt number average becomes larger and especially for a higher value of Raleigh numbers. This could be clarified through the fact of that higher Rayleigh numbers, the rate of the heat transition via radiation convection mode is predominant and becomes more promoted at a higher radiation parameter. It is also very important to observe that the Nusselt number average for (ϕ = 0.04) is the highest.

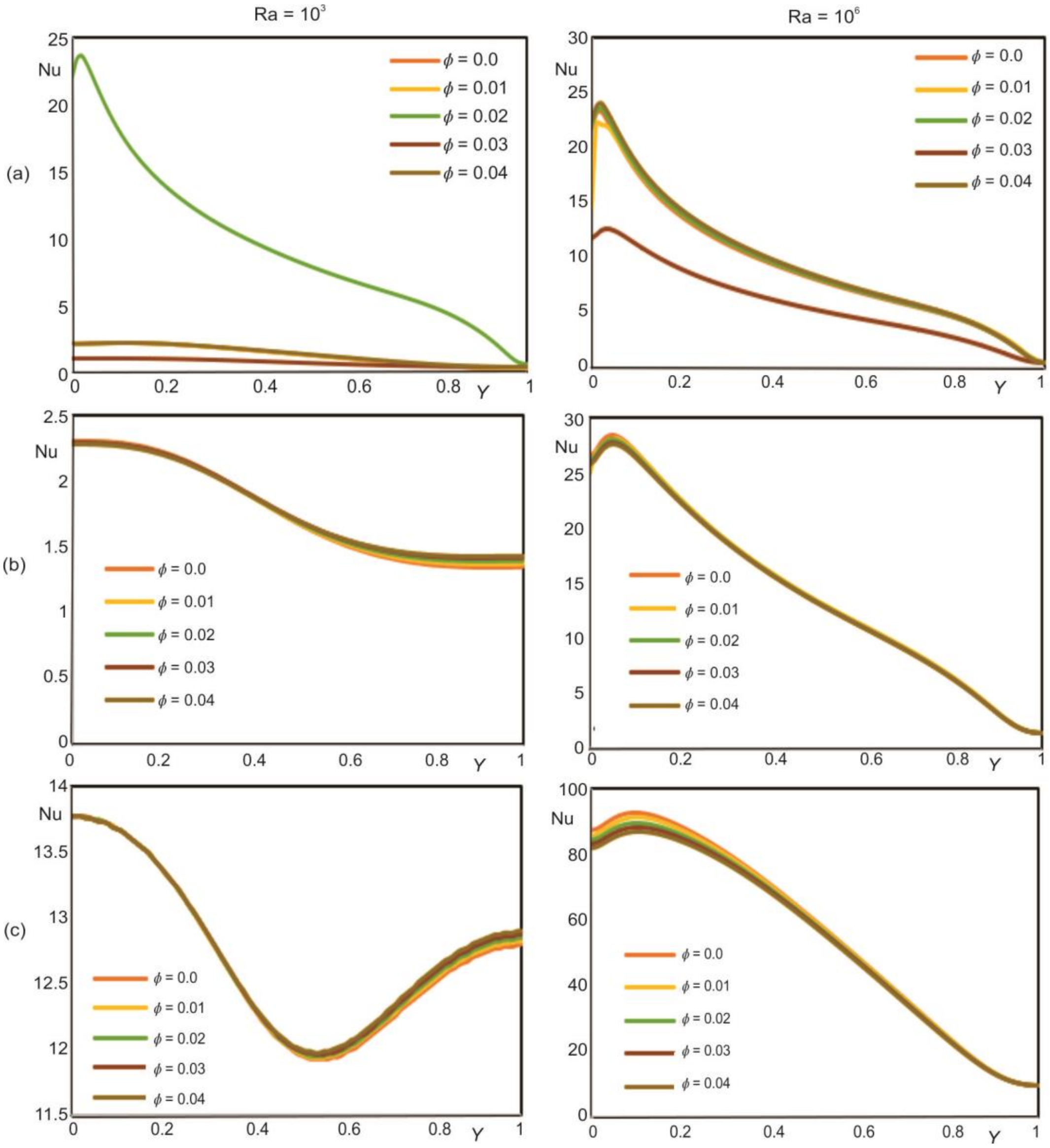

Figure 5. Local Nusselt number for different values of ϕ with; (a) *Rd* = 0, (b) *Rd* = 1, and (c) *Rd* = 10 for Ra = 10^3 and10^6 (*for colour image see journal web site*)

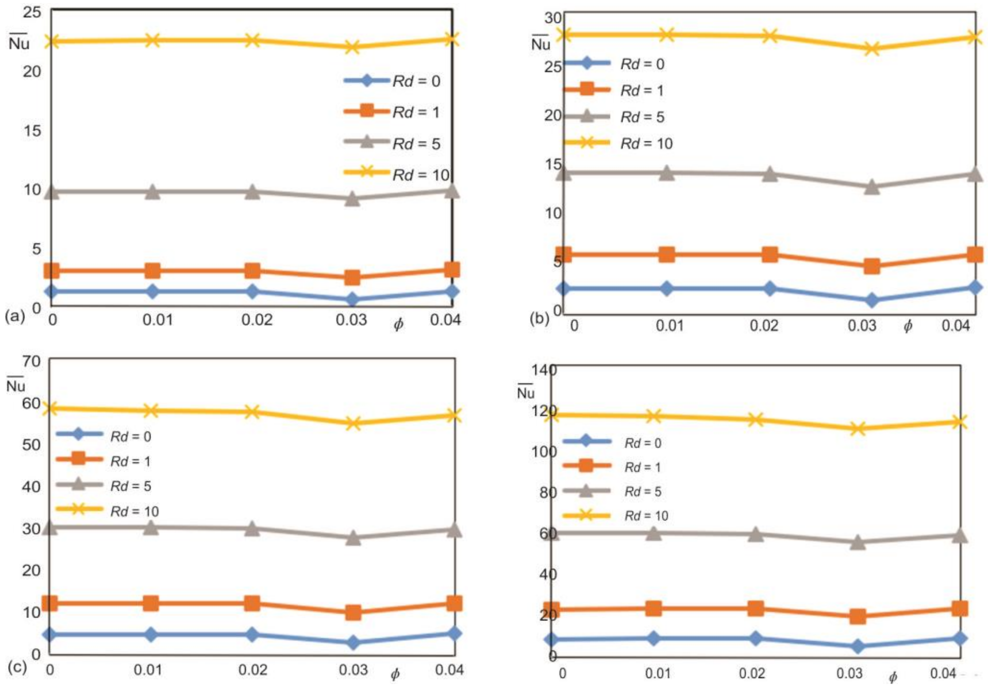

Figure 6. Average Nusselt number for different values of ϕ at various Rayleigh numbers; (a) Ra = 10^3, (b) Ra = 10^4, (c) Ra = 10^5, and (d) Ra = 10^6

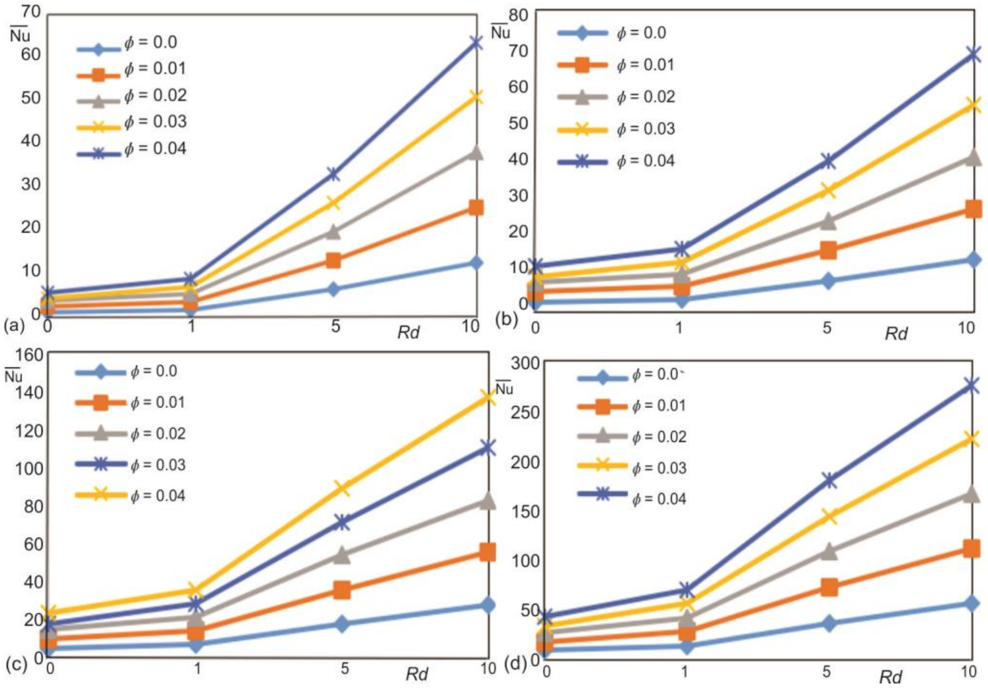

Figure 7. Average Nusselt number for different values of *Rd* at various Rayleigh numbers; (a) Ra = 10^3, (b) Ra = 10^4, (c) Ra = 10^5, and (d) Ra = 10^6

Conclusion

In this study, numerical solutions have been gotten for the influences of the radiation heat transfer with free convection of a Cu-water nanofluid inside a differentially heated enclosure containing an insulated square of height, *ly*, and width, *lx* ($ly = lx = 0.2$) placed in the centre. Finite difference method is used to solve the governing equations and boundary conditions. Based on the overall findings of this study, the following conclusions are drawn as follows.

- The rate of the heat transition increases by increment of the Rayleigh number when the volume part of the nanoparticles is kept constant.
- The average Nusselt number increases by increment in the nanoparticles volume fraction, when the number of Rayleigh is kept constant.
- The streamlines and the isotherms of the changing of the radiation loaded with pure water ($\phi = 0.0$) and Cu-water nanofluid with volume ($\phi = 0.04$) for Ra = 10^6, gives the same conduct for pure fluid (water) and Cu-water nanofluid. The isotherms show that the change of the radiation parameter does not influence the distribution of temperature significantly.
- The variation in the transition of the heat, by employing different nanofluids, rises with the increment of Rayleigh number and nanoparticles volume fraction.
- With an increment in the value of the thermal radiation and the nanoparticles volume fraction, the Nusselt number raises.
- The thermal radiation report $Rd = 10$ gives better Nusselt Number, followed by $Rd = 5$. For all values of the nanoparticles volume fraction, it was almost the same values.
- The influence of the radiation becomes more important with the radiation parameter incremented due to the increased of the transferred of radiative heat to the fluid.

Nomenclature

c_p – specific heat [$\mathrm{Jkg^{-1}K^{-1}}$]
g – gravitational acceleration [$\mathrm{ms^{-2}}$]
H – enclosure height [m]
k – thermal conductivity [$\mathrm{Wm^{-1}K^{-1}}$]
K' – mean absorption coefficient
lx – width of the adiabatic square body [m]
ly – height of the adiabatic square body [m]
Nu – Nusselt number [–]
$\overline{\mathrm{Nu}}$ – average Nusselt number [–]
p – pressure [$\mathrm{Nm^{-2}}$]
$\vec{p}$ – momentum
P – dimensionless pressure [–]
Pr – Prandtl number [–]
q_r – radiation heat flux [$\mathrm{Wm^{-2}}$]
Ra – Rayleigh number [–]
Rd – thermal radiation [$\mathrm{kgm^{-2}}$]
T – dimensional temperature [K]
u, v – dimensional velocities components in x- and y-direction [$\mathrm{ms^{-1}}$]
U, V – dimensionless velocities components in X- and Y-direction [–]
x, y – cartesian co-ordinates [m]
X, Y – dimensionless Cartesian co-ordinates [–]

Greek symbols

α – thermal diffusivity [$\mathrm{m^2s}$]
β – volumetric coefficient of thermal expansion [$\mathrm{K^{-1}}$]
μ – dynamic viscosity [$\mathrm{kgm^{-1}s}$]
ν – kinematic viscosity [$\mathrm{m^2s}$]
ω – vorticity [$\mathrm{s^{-1}}$]
Ω – dimensionless vorticity [–]
ψ – stream function [–]
Ψ – dimensionless stream function [–]
ρ – density [$\mathrm{kgm^{-3}}$]
σ^* – Stefan-Boltzmann constant [$\mathrm{kgm^{-2}\,K^{-4}}$]
Θ – dimensionless temperature [–]
ϕ – Volume fraction of the nanoparticles [–]

Subscripts

c – cold
f – fluid
h – hot
nf – nanofluid

References

[1] Choi, S. U., Eastman J. A., *Enhancing Thermal Conductivity of Fluids with Nanoparticles*, Argonne National Lab., Lemont, Ill, USA, 1995
[2] Hussein, A. K., *et al.*, Three-Dimensional Unsteady Natural Convection and Entropy Generation in an Inclined Cubical Trapezoidal Cavity with an Isothermal Bottom Wall, *Alexandria Engineering Journal, 55* (2016), 2, pp. 741-755
[3] Shen, Z. G., *et al.,* Effect of Tilt Angle on the Stability of Free Convection Heat Transfer in an Upward-Facing Cylindrical Cavity: Numerical Analysis, *International Journal of Thermal Sciences, 107* (2016), Sept., pp. 13-24
[4] Bilgen, E., Oztop, H., Natural Convection Heat Transfer in Partially Open Inclined Square Cavities, *International Journal of Heat and Mass Transfer, 48* (2005), 8, pp. 1470-1479
[5] Iwatsu, R., *et al.,* Mixed Convection in a Driven Cavity with a Stable Vertical Temperature Gradient, *International Journal of Heat and Mass Transfer, 36* (1993), 6, pp. 1601-1608
[6] Cheong, H. T., *et al.,* Natural Convection in a Wavy Porous Cavity with Sinusoidal Heating and Internal Heat Generation, *International Journal of Numerical Methods for Heat & Fliud-flow, 27* (2017), 2, pp. 287-309
[7] Hayat, T., *et al.,* Mixed Convective Three-Dimensional Flow of Williamson Nanofluid Subject to Chemical Reaction, *International Journal of Heat and Mass Transfer, 127* (2018), Part A, pp. 422-429
[8] Hayat, T., *et al.,* Radiative Flow of Micropolar Nanofluid Accounting Thermophoresis and Brownian Moment, *International Journal of Hydrogen Energy*, *42* (2017), 26, pp. 16821-16833
[9] Khan, M. I., *et al.,* Behavior of Stratification Phenomenon in Flow of Maxwell Nanomaterial with Motile Gyrotactic Microorganisms in the Presence of Magnetic Field, *International Journal of Mechanical Sciences, 131-132,* (2017), Oct., pp. 426-434
[10] Hayat, T., *et al.*, Entropy Generation in Flow with Silver and Copper Nanoparticles, *Colloids and Surfaces A: Physicochemical and Engineering Aspects, 539* (2018), Feb., pp. 335-346
[11] Khanafer, K., *et al.,* Buoyancy-Driven Heat Transfer Enhancement in a Two-Dimensional Enclosure Utilizing Nanofluids, *Int. journal of Heat and Mass Transfer 46* (2003), 19, pp. 3639-3653
[12] Sivasankaran, S., *et al.,* Natural Convection of Nanofluids in a Cavity with Linearlyvarying Wall Temperature, *Maejo International Journal of Science and Technology*, *4* (2010), 3, pp. 468-482
[13] Tiwari, R. K., Das, M. K., Heat Transfer Augmentation in a Two-Sided Lid-Driven Differentially Heated Square Cavity Utilizing Nanofluids, *Int. Journal of Heat and Mass Transfer 50* (2018), 9-10, pp. 2002-2018
[14] Hayat, T., *et al.*, Numerical Simulation for Melting Heat Transfer and Radiation Effects in Stagnation Point Flow of Carbon-Water Nanofluid, *Computer methods in applied mechanics and engineering, 315,* (2017), Mar., pp. 1011-1024
[15] Hayat, T., *et al.*, Stagnation Point Flow with Cattaneo-Christov Heat Flux and Homogeneous-Heterogeneous Reaction,. *Journal of Molecular Liquids, 220,* (2016), Aug., pp. 49-55
[16] Hayat, T., *et al.*, Thermally Stratified Stretching Flow with Cattaneo-Christov Heat Flux, *International Journal of Heat and Mass Transfer, 106,* (2017), Mar., pp. 289-294
[17] Hayat, T., *et al.,* Impact of Cattaneo-Christov Heat Flux Model in Flow of Variable Thermal Conductivity Fluid Over a Variable Thicked Surface, *International Journal of Heat and Mass Transfer, 99,* (2016), Aug., pp. 702-710
[18] Hayat, T., *et al.,* Mathematical Modeling of Non-Newtonian Fluid with Chemical Aspects: A New Formulation and Results by Numerical Technique, *Colloids and Surfaces A: Physicochemical and Engineering Aspects, 518,* (2017), Apr., pp. 263-272
[19] Farooq, M., *et al.,* MHD Stagnation Point Flow of Viscoelastic Nanofluid with Non-Linear Radiation Effects, *Journal of molecular liquids, 221,* (2016), Sept., pp. 1097-1103
[20] Khan, M. I., *et al.,* A Comparative Study of Casson Fluid with Homogeneous-Heterogeneous Reactions, *Journal of colloid and interface science, 498* (2017), July, pp. 85-90
[21] Qayyum, S., *et al.,* A Framework for Nonlinear Thermal Radiation and Homogeneous-Heterogeneous Reactions Flow Based on Silver-Water and Copper-Water Nanoparticles: A Numerical Model for Probable Error, *Results in physics, 7,* (2017), June, pp. 1907-1914
[22] Khan, M. I., *et al.,* Entropy Optimization and Quartic Autocatalysis in MHD Chemically Reactive Stagnation Point Flow of Sisko Nanomaterial, *International Journal of Heat and Mass Transfer, 127,* (2018), Part C, pp. 829-837

[23] Hayat, T., *et al.*, New Thermodynamics of Entropy Generation Minimization with Nonlinear Thermal Radiation and Nanomaterials, *Physics Letters A, 382*, (2018), 11, pp. 749-760
[24] Sivasankaran, S., *et al.*, MHD Mixed Convection of Cu-Water Nanofluid in a Two-Sided Lid-Driven Porous Cavity with a Partial Slip, *Numerical Heat Transfer 70* (2016), 12, pp. 1356-1370
[25] Goodarzi, M., *et al.*, Investigation of Heat Transfer and Pressure Drop of a Counter Flow Corrugated Plate Heat Exchanger Using MWCNT Based Nanofluids, *Int. communications in heat and mass transfer 66* (2015), Aug., pp.172-179
[26] Esfe, M. H., *et al.*, Numerical Simulation of Natural Convection Around an Obstacle Placed in an Enclosure Filled with Different Types of Nanofluids, *Heat Transfer Research 45* (2014), 3, pp. 279-292
[27] Hayat, T., *et al.*, Entropy Generation in Magnetohydrodynamic Radiative Flow Due to Rotating Disk in Presence of Viscous Dissipation and Joule Heating, *Physics of Fluids, 30*, (2018), 1, 017101
[28] Karimipour, A., New Correlation for Nusselt Number of Nanofluid with $Ag/Al_2O_3/Cu$ Nanoparticles in a Microchannel Considering Slip Velocity and Temperature Jump by Using Lattice Boltzmann Method, *Int. Journal of Thermal Sciences 91* (2015), May, pp. 146-146
[29] Md Kasmani, R., *et al.*, Analytical and Numerical Study on Convection of Nanofluid Past a Moving Wedge with Soret and Dufour Effects, *Int. Journal of Numerical Methods for Heat & Fliud-flow 27* (2017), 10, pp. 2333-2354
[30] Elbashbeshy, E. M., *et al*., Effects of Thermal Radiation and Magnetic Field on Unsteady Mixed Convection Flow and Heat Transfer Over an Exponentially Stretching Surface with Suction in the Presence of Internal Heat Generation/Absorption, *Journal of the Egyptian Mathematical Society, 20* (2012), 3, pp. 215-222
[31] Safaei, M. R., *et al.*, The Investigation of Thermal Radiation and Free Convection Heat Transfer Mechanisms of Nanofluid Inside a Shallow Cavity by Lattice Boltzmann Method, *Physica A: Statistical Mechanics and its Applications 509* (2018), Nov., pp. 515-535
[32] Ridouane, E. H., *et al.*, Interaction Between Natural Convection and Radiation in a Square Cavity Heated from Below, *Numerical Heat Transfer, Part A: Applications 45* (2004), 3, pp. 289-311
[33] Ridouane, E. H., *et al.*, Effects of Surface Radiation on Natural Convection in a Rayleigh-Bénard Square Enclosure: Steady and Unsteady Conditions, *Heat and mass transfer, 42* (2006), 3, 214-225
[34] Kogawa, T., Influence of Radiation Effect on Turbulent Natural Convection in Cubic Cavity at Normal Temperature Atmospheric Gas, *Int. Journal of Heat and Mass Transfer, 104* (2017), Jan., pp. 456- 466
[35] Alsabery, A., Effects of Finite Wall Thickness and Sinusoidal Heating on Convection in Nanofluid-Saturated Local Thermal Non-Equilibrium Porous Cavity, *Physica A: Statistical Mechanics and its Applications 470* (2017), Mar., pp. 20-38
[36] De Vahl Davis, G., Jones, I., Natural Convection in a Square Cavity, *International Journal for Numerical Methods in Fluids, 3* (1983), 3, pp. 249-264
[37] Bilgen, E., Yeder, R. B., Natural Convection in Enclosure with Heating and Cooling by Sinusoidal Temperature Profiles on One Side, *International Journal of Heat and Mass Transfer, 50* (2007), 1-2, pp. 139-150
[38] Ho, C. J., *et al.*, Numerical Simulation of Natural Convection of Nanofluid in a Square Enclosure: Effects Due to Uncertainties of Viscosity and Thermal Conductivity, *International Journal of Heat and Mass Transfer, 51* (2008), 17-18, pp. 4506-4516
[39] Cheong, H., *et al.*, Effect of Aspect Ratio on Natural Convection in an Inclined Rectangular Enclosure with Sinusoidal Boundary Condition, *International Communications in Heat and Mass Transfer, 45* (2013), July, pp. 75-85

Paper submitted: October 3, 2019
Paper revised: March 12, 2020
Paper accepted: May 25, 2020